Supporting Information

Nanoparticles modified with glucose analogs to enhance the permeability of the blood-brain barrier and its accumulation in epileptic brain

Qian Meng, [a] *Xiaoyu Zhang,*[a, b] *Yuwen Chen,* [a] *Hao Yang,* [c] *Jinshuai Liu,* [a] *Zifan Yang,* [a] *Jianxiang Lei,* [a] *Fengqing Lu,* [a] *Dengyuan Hao,* [e] *Lijie Feng,**[, c, d] *and Yu Wang**[, a, b]

[a] Department of Neurology, the First Affiliated Hospital of Anhui Medical University, Hefei 230022, Anhui, P. R. China

[b] Anhui Public Health Clinical Center, Hefei 230022, Anhui, P. R. China.

[c] School of Basic Medical Sciences, Anhui Medical University, Hefei 230022, Anhui, P. R. China

[d] Biopharmaceutical Research Institute, Anhui Medical University, Hefei 230022, Anhui, P. R. China

[e] State Key Laboratory of Polymer Physics and Chemistry, Changchun Institute of Applied Chemistry, Chinese Academy of Sciences, Changchun 130022, Jilin, P. R. China

*E-mail address: yw4d@hotmail.com, fenglijie1128@sina.com

Materials

2-deoxy-2-amino-D-glucose hydrochloride (2-DG) and IR780 were purchased from Energy Chemical Co., Ltd.. 1,2-distearoyl-sn-glycero-3-phosphoethanolamine-N-[methoxy(polyethylene glycol)2000] (DSPE-PEG_{2K}) and 1,2-distearoyl-sn-glycero-3-phosphoethanolamine-N-[Succinimidyl Succinate ester (polyethylene glycol)2000] (DSPE-PEG_{2K}-NHS) were purchased from Shanghai Ponsure Biological Co., Ltd.. 3-(4,5-dimethylthiazol-2-yl)-2,5-diphenyl-2h-tetrazoliubromide (MTT) was bought from Ambeed Inc.. 4′,6-diamidino-2-phenylindole (DAPI), Dulbecco's Modified Eagle Medium High Glucose (DMEM), and goat anti-mouse IgG Alexa Fluor® 488 were supplied by Wuhan Servicebio Technology Co., Ltd.. DMEM without glucose and Trypsin-EDTA solution (0.25%, without phenol red) were obtained from Beijing Solarbio Methods Science & Technology Co., Ltd.. Dimethyl sulfoxide-d_6 (DMSO-d_6), urea, ethylenediaminetetraacetic acid disodium salt (EDTA), triton X-100 were purchased from Adamas-beta Reagent Co. Ltd.. Dialysis membranes (2000 Da) were purchased from Shanghai Acmec Biochemical Technology Co., Ltd.. Fetal bovine serum (FBS), phosphate buffered saline (PBS, pH 7.4), and Penicillin Streptomycin were obtained from Wuhan Pricella Biotechnology Co., Ltd.. Pilocarpine hydrochloride (Pilo) was obtained from TargetMol Chemicals Inc.. Kainic acid (KA) were supplied by Glpbio Technology Inc. DMSO (AR grade) and acetone (AR grade) were purchased from Xilong Scientific Co., Ltd.. Cell culture bottle, 6-Well plates, 150 mm cell culture dishes,and centrifuge tubes were obtained from NEST Biotechnology Co. Ltd.. Ultrapure water from Millipore Q water purification system was used to prepare all solutions.

Measurements

The prepared compounds were confirmed using a nuclear magnetic resonance spectrometer (AVANCE DRX 500, Bruker) and matrix-assisted laser desorption/ionization time-of-flight mass spectrometry (MALDI-TOF-MS) (Ultraflextreme, Bruker). An analytical balance (GL124i-1SCN, Sartorius) and TopPette pipettes (DLAB scientific) were used for quantification of the solid and liquid, respectively. The morphology of nanoparticles (NPs) was determined by a transmission electron microscope (TEM) (Talos L120C G2, Thermo Fisher Scientific) with an acceleration voltage of 120 kV. ξ-Potential and hydrodynamic diameter of NPs were characterized by Zeta-sizerNano (Nano ZS90, Malvern Panalytical). Ultraviolet absorption was measured by UV-vis spectroscopy (UV-1800, ShiMadzu). Fluorescence emission spectrum was measured by fluorescence spectrophotometer (FS5, Edinburgh). The optical density (OD) value of MTT assay was determined using a microplate reader (BioTek Cytation 5, Agilent). The cellular uptake of NPs was qualitatively observed using fluorescence microscope (DM 6B, Leica) and quantitatively measured on flow cytometry (FCM) (CytoFLEX, Beckman Coulter). The in vivo and in vitro fluorescence images were detected using an in vivo imaging system (IVIS) (Amix, Spectral Instruments Imaging). Automatic biochemical analyzer (3100 Full-automatic biochemical analyzer, Hitachi) was used to measure the clinical parameters. A cryostat microtome (CM1950, Leica) was used to prepare brain coronal slices.

Methods

Synthesis of 2-deoxy-2-amino-D-glucose conjugated DSPE-PEG_{2K} (DSPE-PEG_{2K}-2-DG)

DSPE-PEG_{2K}-2-DG was synthetized by the amidation reaction of DSPE-PEG_{2K}-NHS and 2-DG. In detail, DSPE-PEG_{2K}-NHS (100 mg, 0.034 mmol, 1e.q.) was dissolved in 5 mL acetone and added to 20 mL ultrapure water. Then 2-DG (36 mg, 0.169 mmol, 5e.q.) was added and the mixture was stirred at room temperature for further 48 h. The product was obtained by freeze-dried after dialyzed against ultrapure water using a dialysis membrane (2000 Da) for three days.

Preparation and characterization of nanoparticles

Boron-dipyrromethane (BDP)/IR780-loaded NPs were prepared by nanoprecipitation method.[1, 2] Typically, 0.5 mg BDP and 5 mg DSPE-mPEG_{2K} or DSPE-PEG_{2K}-2-DG were dissolved in 0.2 mL acetone and dropped into 5 mL ultrapure water with a syringe and stirred overnight at room temperature to evaporate the acetone. Then the solution was dialyzed against ultrapure water using a dialysis membrane (2000 Da) for 24h. Finally, the BDP-loaded NPs (B-NNPs and B-GNPs) were obtained. cargo-free NPs (NNPs and GNPs) and IR780-loaded NPs (IR-NNPs and IR-GNPs) were prepared with similar procedure.

The hydrodynamic diameter, polydispersity index (PDI), and ξ-Potential of NPs were determined by dynamic light scattering (DLS), while the morphology was characterized using the TEM at an accelerating voltage of 120 kV. The standard curve of BDP and IR780 was established via UV-vis spectroscopy. Thus, the loading efficiency (LE) and entrapment efficiency (EE) of BDP or IR780 in NPs were determined as

follows:

$$LE\ (wt\%) = \frac{The\ weight\ of\ loaded\ BDP\ or\ IR780}{The\ weight\ of\ NPs} \times 100\%$$

$$EE\ (wt\%) = \frac{The\ weight\ of\ loaded\ BDP\ or\ IR780}{Total\ weight\ of\ BDP\ or\ IR780} \times 100\%$$

In vitro stability and the assembly driving force of nanoparticles

To evaluate the stability of NPs, the hydrodynamic diameter changes of NPs were measured by DLS over a period of fourteen days. NPs were cultured with NaCl, UREA, ethylenediaminetetraacetic acid disodium (EDTA), and Triton X-100 solution, respectively, and then the changes of hydrodynamic diameter distribution and PDI were detected to clarify the driving force of assembly.

Cell culture

Mouse brain microvascular endothelial cells (bEnd.3) and Hippocampal neuronal cells (HT22), purchased from Melone Pharmaceutical Co., Ltd., were maintained in DMEM supplemented with 10% (v/v) FBS and 1% (v/v) Penicillin Streptomycin, respectively. All the cell lines were maintained in a humidified incubator at 37°C, 5% CO_2.

Cell viability assay

To evaluate the cytotoxicity of DSPE-PEG_{2K}-2-DG, the MTT assay was performed. In short, cells (bEnd.3 and HT22 cells) were inoculated in 96-well culture plates and incubated at 37°C overnight, respectively. After adhering, the NNPs and GNPs with different carrier concentrations (0-500 μg mL^{-1}) were added and incubated for further 24 h. Subsequently, 20 μL MTT (5 mg mL^{-1}) was added and cultured for another 4 h. After that, the culture medium was carefully removed and 150 μL DMSO was added

to each well to dissolve the formed violet formazan crystals. Ultimately, the OD value of the violet product at 490 nm wavelength was determined using a microplate reader.

In vitro cellular uptake

To evaluate the internalization of B-NNPs and B-GNPs by cells, bEnd.3 and HT22 cells were seeded in a 6-well plate and allowed to adhere for 24 h, and then cells were treated with B-NNPs and B-GNPs at a BDP concentration of 0.2 μg mL^{-1} for 0.5 h, 1 h, and 4 h, respectively. After washed with PBS (10 mM, pH 7.4) solution three times, cells were fixed with 4% paraformaldehyde for 15 min at room temperature. Subsequently, the cell nuclei were stained with DAPI for 10 min. Finally, cells were washed with PBS (10 mM, pH 7.4) solution three times and the representative images of cells were captured by fluorescence microscopy and fluorescence intensity of bEnd.3 and HT22 cells treated with both NPs was semi-quantified using Image J.

FCM was further adopted to analyze the cellular uptake of B-NNPs and B-GNPs quantitatively. Briefly, bEnd.3 and HT22 cells were seeded in 6-well plates and grown overnight, and then cells were treated with B-NNPs and B-GNPs at a BDP concentration of 0.02 μg mL^{-1} for 0.5 h, 1 h, and 4 h at 37°C, respectively. Subsequently, the cells were trypsinized and centrifuged at RCF 193g (1000 rpm) for 4 min at 4°C after washed with PBS (10 mM, pH 7.4) three times. Then, the cells were resuspended in PBS (10 mM, pH 7.4) to obtain single cell suspension and CytoFLEX was used to measure the fluorescence intensities of samples.

In the competitive binding experiment (2-DG modified NPs/2-DG or glucose), 1 mg

ml^{-1} 2-DG or glucose was added to the wells in advance (bEnd.3 and HT22 cells). After 0.5 h incubation at 37°C, the medium was removed from the wells, and B-GNPs at a BDP concentration of 0.2 μg mL^{-1} was added and incubated for another 1 h. To observe a temperature effect, the cellular incubation (bEnd.3 and HT22 cells) with NPs was carried out at 4°C. The mean fluorescence intensity was semi-quantified using Image J.

The targeting capabilities of GNPs with different ligand densities were further studied. DSPE-$mPEG_{2K}$ and DSPE-PEG_{2K}-2-DG were mixed in different weight proportions to prepare B-GNPs with different surface 2-DG densities (0, 25, 50, 75, and 100%), where BDP was encapsulated as fluorescence probe. bEnd.3 and HT22 cells were treated with B-GNPs with different surface 2-DG densities at a BDP concentration of 0.2 μg mL^{-1} for 4 h. After washed with PBS (10 mM, pH 7.4) solution three times, cells were fixed with 4% paraformaldehyde for 15 min at room temperature. Subsequently, the cell nuclei were stained with DAPI for 10 min. Finally, cells were washed with PBS (10 mM, pH 7.4) solution three times and the representative images of cells were captured by fluorescence microscopy.

In vitro BBB model

To investigate the BBB permeability of nanoparticles, bEnd.3 cells were cultured in the upper chambers of transwell plate (24 wells, pore size: 0,4 μm, Corning, USA) to form a monolayer. The culture medium was refreshed once per day. The trans-endothelial electrical resistance (TEER) was monitored using a TEER instrument (EVOM 3, World Precision Instruments, USA). When the TEER value reached 200 $\Omega \cdot cm^2$, it was

considered that a tight monolayer of cells had formed.[3] Then B-NNPs and B-GNPs were added to upper chambers and incubated with cells for 24h. A volume of 200 μl sample medium was taken from the basolateral compartment at 1, 2, 4, 8, 12 and 24 h, and replaced with an equal volume of fresh medium. The BDP contents of in sample were determined by microplate reader (EnSpire, PerkinElmer). The transport ratio of B-NNPs and B-GNPs was calculated with the formula: ratio=(Wn/W) ×100, where Wn is the BDP amounts of samples taken from basal chamber at the nth h (n= 1, 2, 4, 8, 12 and 24 h), and W is the BDP amount of control added in apical chamber. At the end of the experiment, TEER was measured again to monitor the integrity of bEnd.3 cells monolayers.

Animals

Male C57BL/6J (6-8 weeks) with body weight of 22-25 g were provided by Gempharmatech Co., Ltd. (SCXK[Su] 2023-0009, Suzhou, China). Animals were maintained under controlled environmental conditions (20-24°C) with relative humidity at 50-60% and 12-h light/dark period. All animals were free access with water and food throughout the experiment. And all animal experiments were reviewed and approved (Approved No. 20200470) by the Committee on the Ethics of Animal Experiments of The First Affiliated Hospital of Anhui Medical University, China.

Pilocarpine-induced status epilepticus

The Pilocarpine-induced epileptic model was established in C57BL/6J mice according to previously described procedures.[4-6] In brief, all C57BL/6J mice were received an intraperitoneal (i.p.) injection of pilocarpine (200 to 300 mg kg^{-1} i.p.). To minimize the

peripheral effects of cholinergic stimulation, mice were injected scopolamine (1 mg kg^{-1} i.p.) 30 min before pilocarpine administration. Behavioral seizures of all mice were classified into five stages: (i) mouth and facial movements. (ii) chewing and head nodding. (iii) unilateral forelimb clonus. (iv) bilateral forelimb clonus with rearing. (v) continuous rearing and falling.

Kainic acid-induced status epilepticus

Kainic acid-induced epilepticus model was established in C57BL/6J mice by intraperitoneally injections of kainic acid (KA, 18-22 mg mL^{-1}) dissolved in 0.9% saline according to a previously described protocol.[7, 8] Seizure behavior was monitored in accordance with Racine's scale as mentioned above.

Evaluation of targeting ability in vivo

To study the BBB penetration of 2-DG-modified NPs, IR-NNPs and IR-GNPs were intravenously injected to heathy C57BL/6J mice. During the next 24 h, mice were anesthetized and visualized by Spectral Instruments Imaging system at 0 h, 1 h, 3 h, 7 h,12 h, and 24 h. The fluorescence intensity of IR780 of mice head was subsequently quantified by region of interest (ROI) analysis.

To further study the cerebral distribution of 2-DG-modified NPs, mice were intravenously injected with IR-NNPs and IR-GNPs and established pilocarpine and KA-induced SE of C57BL/6J mice. At the fourth hour post-injection with saline and NPs, mice were anaesthetized and transcardially perfused with saline (0.9%, v/v). After that, the whole brains of mice were collected and the fluorescence intensity was analyzed using IVIS. The fluorescence intensity of IR780 of mice brain was

subsequently quantified by region of interest (ROI) analysis.

IR-NNPs and IR-GNPs were intravenously injected to healthy and epileptic mice, respectively. After 4 hours, the mice were sacrificed and the brains were collected to prepare 20-μm-thick frozen coronal sections for examining the accumulation of nanoparticles in neurons. For immunofluorescence staining, slices were washed with PBS (10 mM, pH 7.4) three times and were blocked by QuickBlock™ blocking buffer (Beyotime, China) for 1 h at 37 ^{o}C. Then the slices were incubated with primary antibody (anti-neuron, 1:400) at 4 ^{o}C overnight. The next day, brain slices were washed with PBS (10 mM, pH 7.4) five times and incubated with secondary antibody (goat anti-mouse IgG Alexa Fluor® 488, 1:400) for 1 h at 37 °C. After washed with PBS (10 mM, pH 7.4) five times, the slices were stained with DAPI for 10 min. Finally, brain slices were imaged using a fluorescence microscope.

Blood compatibility

The blood compatibility of IR-NNPs and IR-GNPs was evaluated by a hemolysis assay.[9] In brief, the whole blood was collected into heparinized tubes and centrifuged at RCF of 433 g (1500 rpm) for 10 min, and then washed with saline (0.9%, v/v) until the supernatant is colorless to obtain pure erythrocytes. Then IR-NNPs and IR-GNPs were mixed with 5% erythrocytes (v/v) suspension and incubated for 1 h at 37°C. The ultrapure water and saline (0.9%, v/v) were used as positive and negative controls, respectively. After incubating, the samples were centrifuged at RCF of 433 g (1500 rpm) for 5 min. The absorbance of supernatant was measured at 540 nm, and the hemolysis was calculated by the formula below.

$$Hemolysis(\%) = \frac{OD_{sample} - OD_{negative\ control}}{OD_{positive\ control} - OD_{negative\ control}} \times 100$$

Open-field test

The open-field test was performed to evaluate general motor activity and anxiety-like behavior in animals administrated with saline and IR780-loaded NPs by using an open-field apparatus (50×50×50 cm).[10] The center zone was defined as a square. All animals were habituated to the experimental environment for 30 min and were allowed to familiarize themselves with open-field apparatus for 5 min. Afterwards, each animal was placed in the apparatus to start test and recorded using a video tracking system for 10 min. The box was cleaned with 75% alcohol solution after each test. The motion route of each animal was captured, and the total distance and average speed were measured.

Novel object recognition test

The novel object recognition test was performed to access recognition memory according to previous described.[11] In brief, animals were placed in an open-field apparatus (50×50×50 cm) for 10 min. Two identical objects were placed on the bottom of the box and located in opposite and equidistant positions after 24 h. Then, the mice were allowed to freely explore these two objects for 10 min. After an hour, one of the familiar objects was replaced by a novel object, and each mouse was allowed to explore for another 5 min. The exploratory preference was evaluated by the ratio of the time spent in exploring novel objects and time spent in exploring the two objects. The box was cleaned after each test to eliminate the presence of olfactory trials.

Biosafety evaluation

To assess the safety of IR-NNPs and IR-GNPs in vivo, heathy C57BL/6J mice were assigned randomly into three groups and were administrated intravenously with saline and IR780-loaded NPs. On day 7, the serum of mice was collected by centrifuging the blood at RCF of 1734 g (3000 rpm) for 10 min, following the biochemical parameters including aspartate aminotransferase (AST), alanine aminotransferase (ALT), creatinine (CREA) and urea (UREA) were analyzed using a full-automatic biochemical analyzer. And then, the major organs (heart, liver, spleen, lung, and kidney) were collected and fixed in 4% paraformaldehyde solution. Subsequently embedded in paraffin, sliced, and stained with hematoxylin and eosin (H&E) to evaluate potential toxicity of IR780-loaded NPs.

Statistical analysis

All data were expressed as mean ± standard deviation (SD). The statistical significance among the groups was calculated by comparing their means through one-way ANOVA or two-way ANOVA. Statistical significance was calculated as $*P < 0.05$, $**P < 0.01$, $***P < 0.001$, and $****P < 0.0001$.

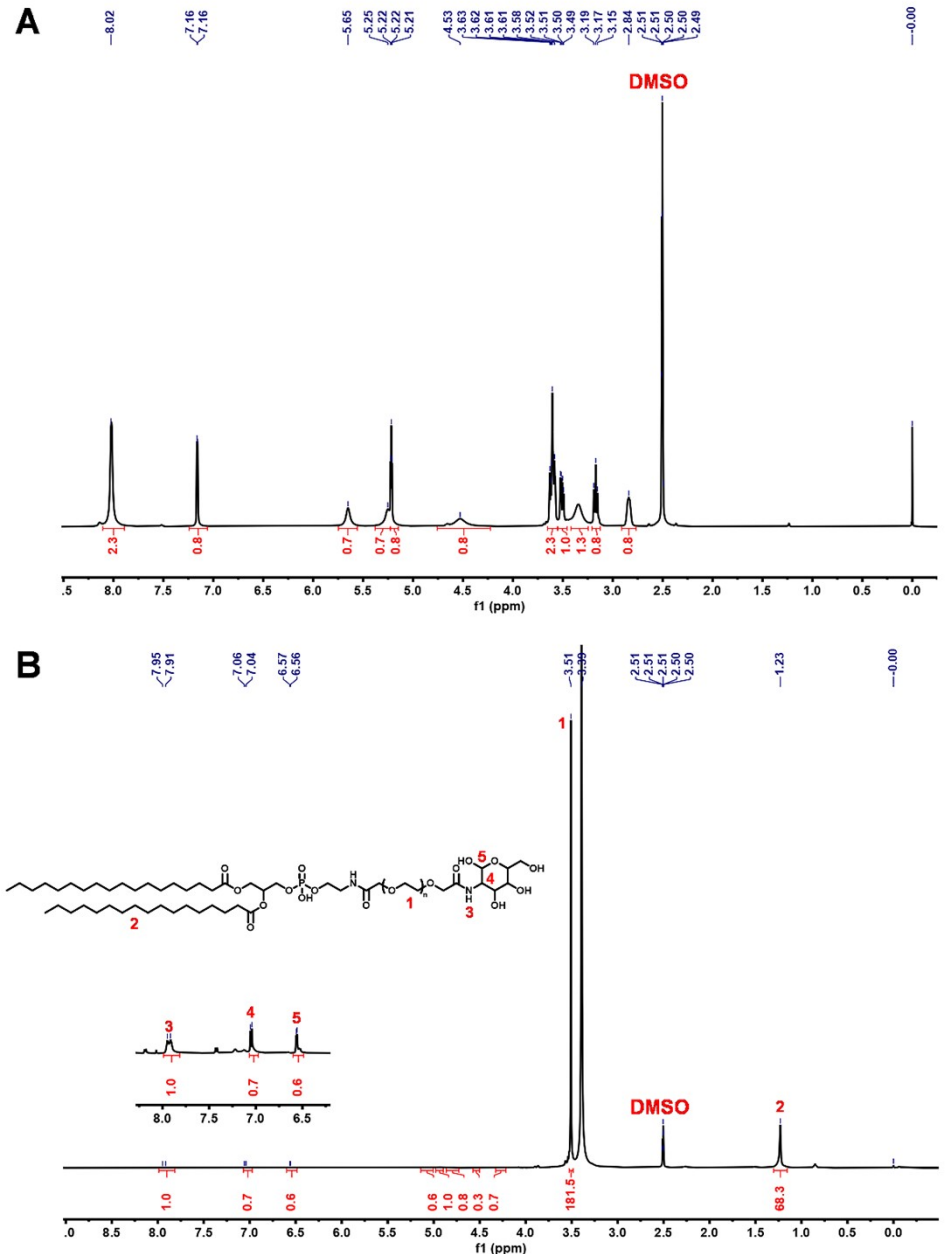

Figure S1. ^{1}H NMR spectra of 2-deoxy-2-amino-D-glucose hydrochloride (A) and DSPE-PEG$_{2k}$-2-DG (B) in DMSO-d$_6$.

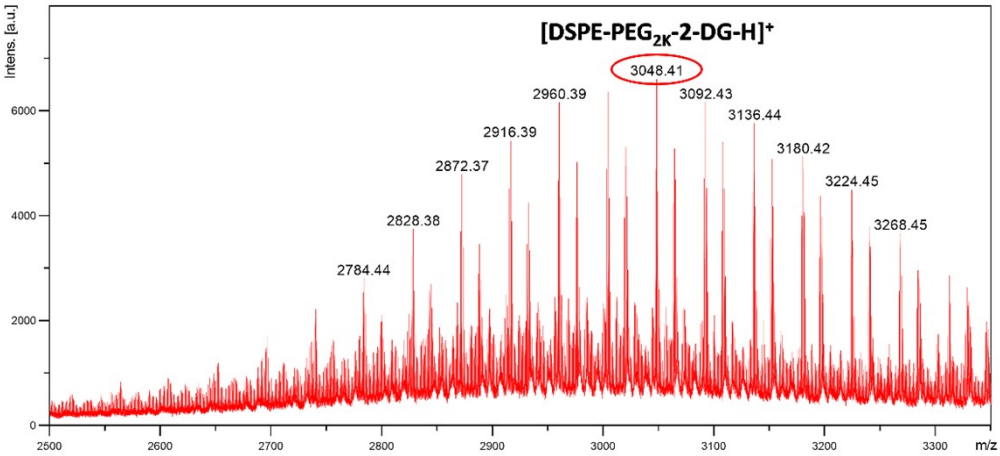

Figure S2. MALDI-TOF-MS analysis of DSPE-PEG_{2K}-2-DG.

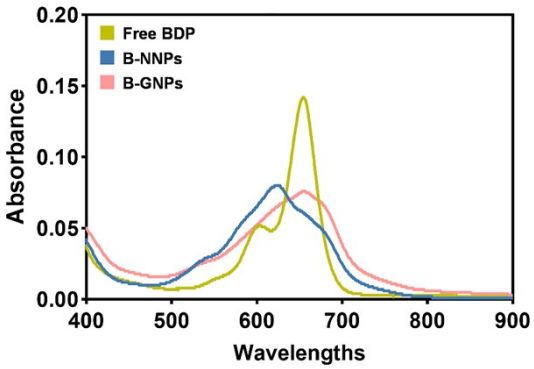

Figure S3. Absorption spectra of free BDP, B-NNPs, and B-GNPs at equivalent BDP concentration.

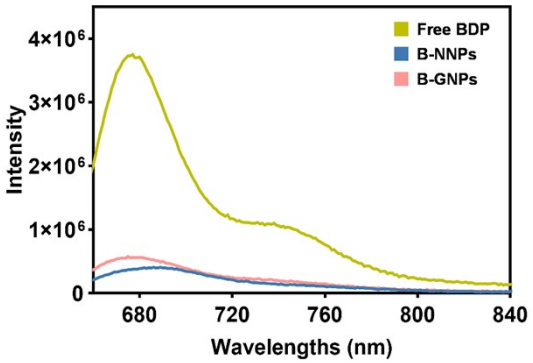

Figure S4. Fluorescence spectra of free BDP in the mixed solutions of DMSO and H_2O (9/1, v/v), B-NNPs and B-GNPs in H_2O at equivalent BDP concentration.

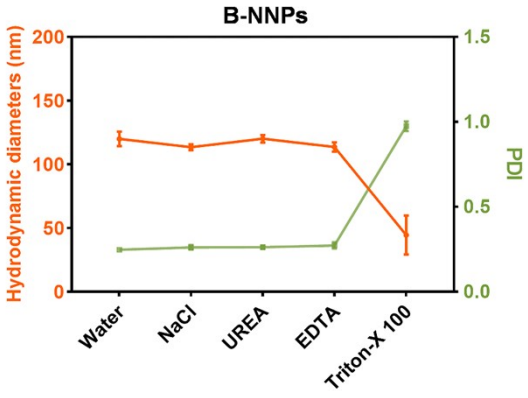

Figure S5. The variation of hydrodynamic diameters and PDI of B-NNPs incubated with ultrapure water, NaCl, UREA, EDTA and Triton X-100. Bars express SD (n = 3).

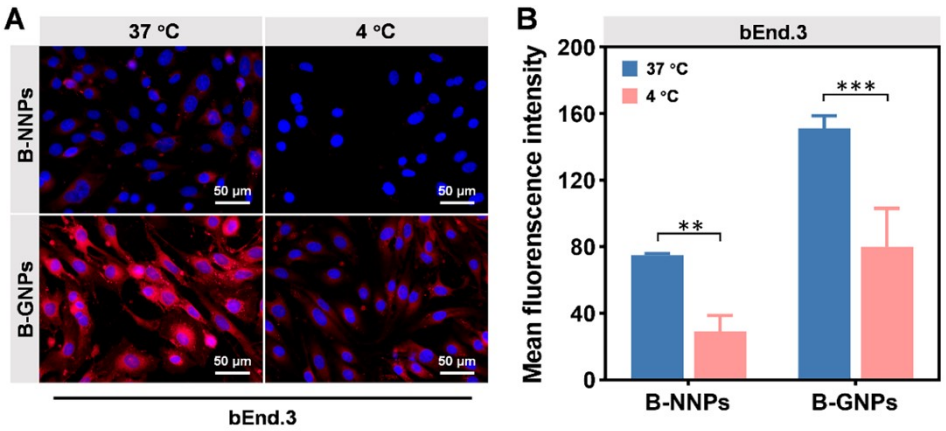

Figure S6. Fluorescence microscopy images (A) and corresponding intracellular fluorescence intensities quantification (B) of bEnd.3 cells cultured with B-NNPs and B-GNPs at 37°C and 4°C. Scale bars: 50 μm. Bars express SD (n = 3). The significant difference was detected by two-way ANOVA. Statistical P-values: **P < 0.01, ***P < 0.001.

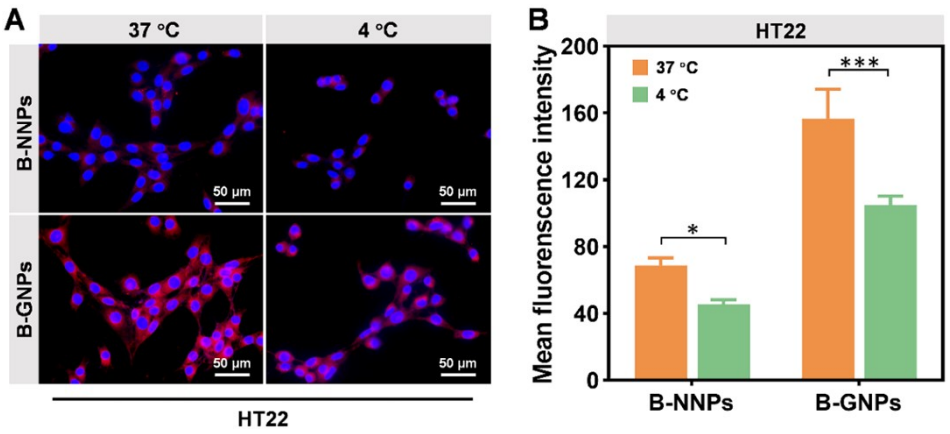

Figure S7. Fluorescence microscopy images (A) and corresponding intracellular fluorescence intensities quantification (B) of HT22 cells cultured with B-NNPs and B-GNPs at 37°C and 4°C. Scale bars: 50 μm. Bars express SD (n = 3). The significant difference was detected by two-way ANOVA. Statistical P-values: *P < 0.05, ***P < 0.001.

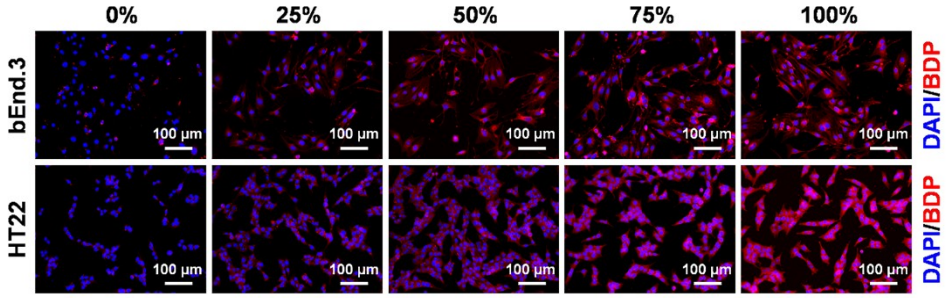

Figure S8. Fluorescence microscopy images of bEnd.3 and HT22 cell cultured with B-GNPs containing different proportions of DSPE-PEG_{2K}-2-DG (0, 25, 50, 75, and 100%) at 37°C for 4h. Scale bars, 100 μm.

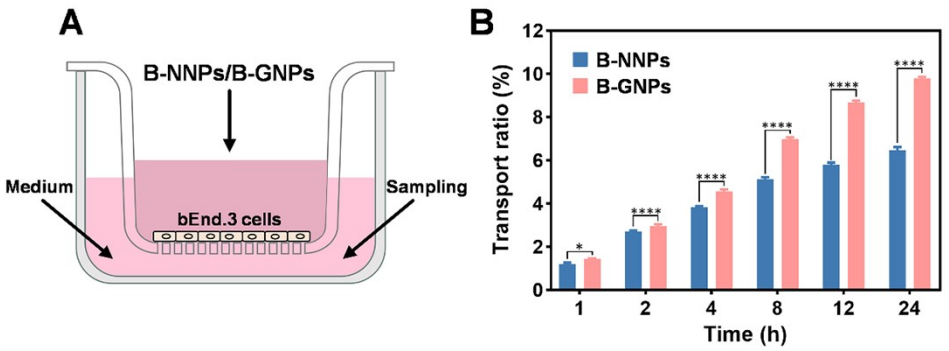

Figure S9. (A) Schematic diagram of the BBB model in vitro. (B) Quantitative transcytosis of B-NNPs or B-GNPs across the BBB model in vitro. Bars express SD (n = 3). The significant difference was detected by two-way ANOVA. Statistical P-values: *P < 0.05, ****P < 0.0001.

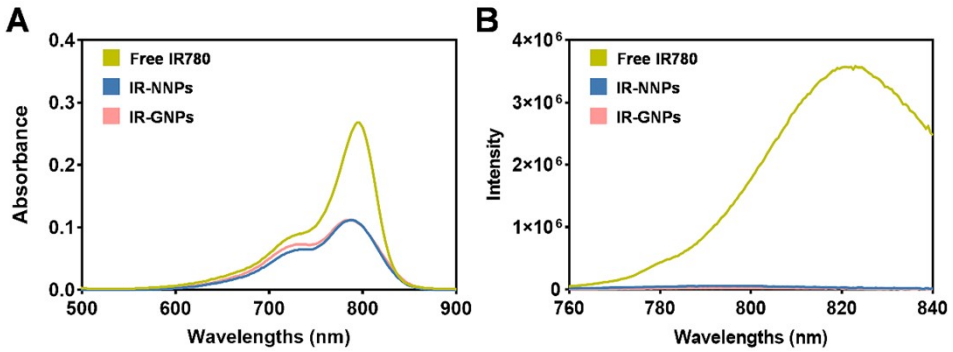

Figure S10. (A) Absorption spectra of free IR780 in DMSO and H_2O (9/1, v/v), IR-NNPs and IR-GNPs at equivalent IR780 concentration. (B) Fluorescence spectra of free IR780 in the mixed solutions of DMSO and H_2O (9/1, v/v), IR-NNPs and IR-GNPs in H_2O at equivalent IR780 concentration.

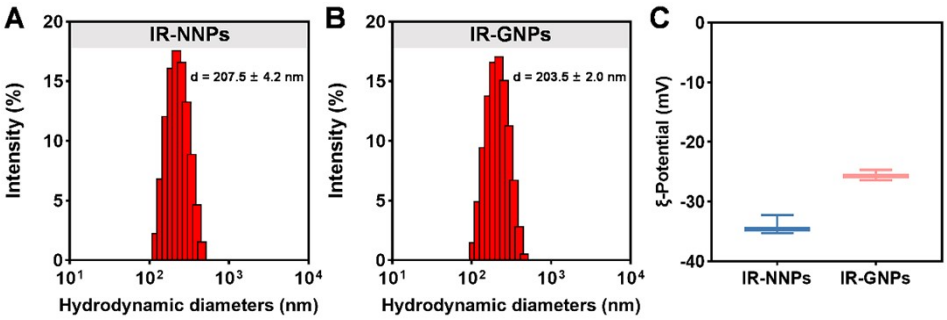

Figure S11. Hydrodynamic diameters distribution of IR-NNPs (A) and IR-GNPs (B). (C) ξ-Potential results of IR-NNPs and IR-GNPs. Bars express SD (n = 3).

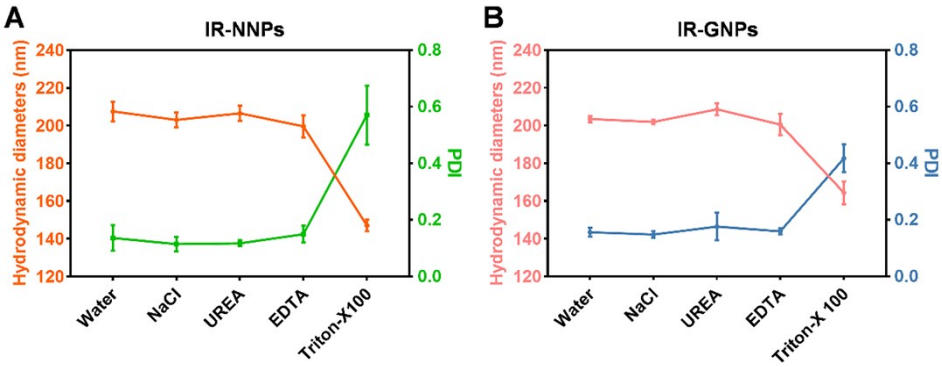

Figure S12. Hydrodynamic diameters and PDI changes of IR-NNPs (A) and IR-GNPs (B) after being treated with deionized water, NaCl, urea, EDTA, and Triton X-100 solutions. Bars express SD (n = 3).

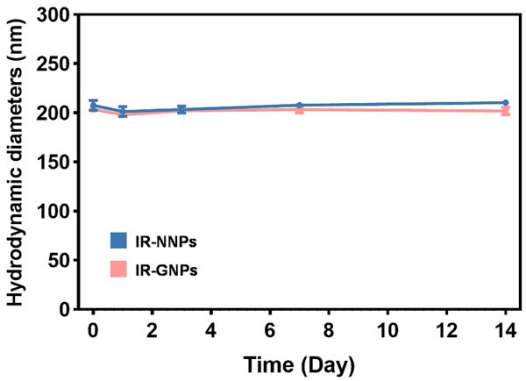

Figure S13. Hydrodynamic diameter changes of IR-NNPs and IR-GNPs in ultrapure water at different times. Bars express SD (n = 3).

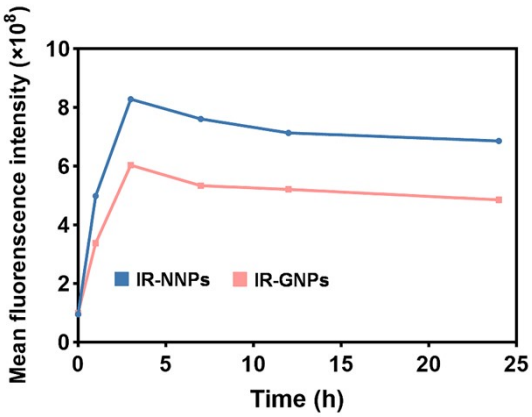

Figure S14. Quantified data of fluorescence signal of the brain in healthy mice treated with IR-NNPs and IR-GNPs. (Unit of the intensity: Photons/s/cm^2/sr)

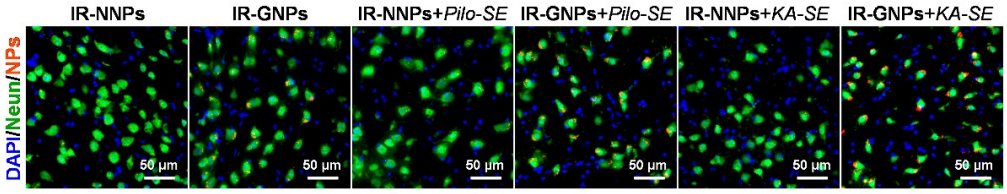

Figure S15. Slices of mouse brain after injection with IR-NNPs or IR-GNPs for 4h (blue: DAPI; green: Neurons; red: IR-780). Scale bar: 50 μm.

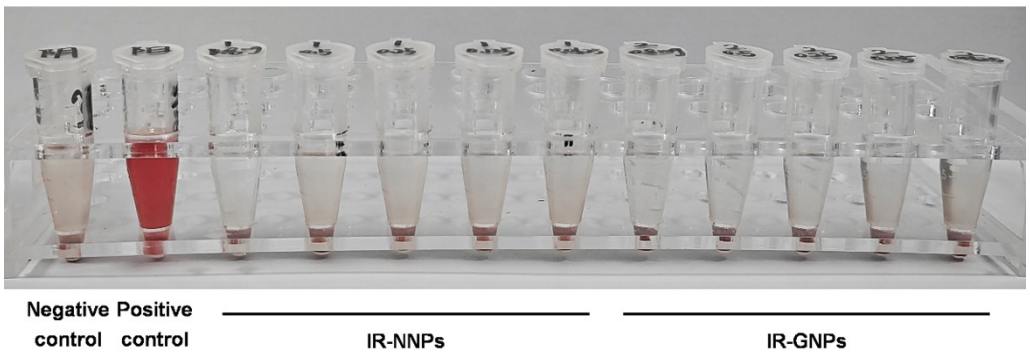

Figure S16. The hemolysis experiment images of IR-NNPs and IR-GNPs with different concentrations.

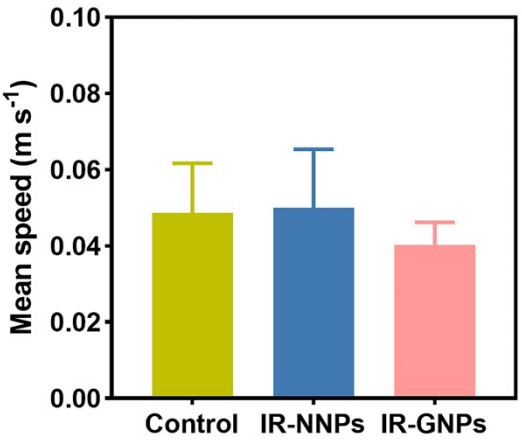

Figure S17. Mean speed of spontaneous motion in an open-field test of the mice after intravenous injection of saline, IR-NNPs and IR-GNPs. Bars express SD (n = 3).

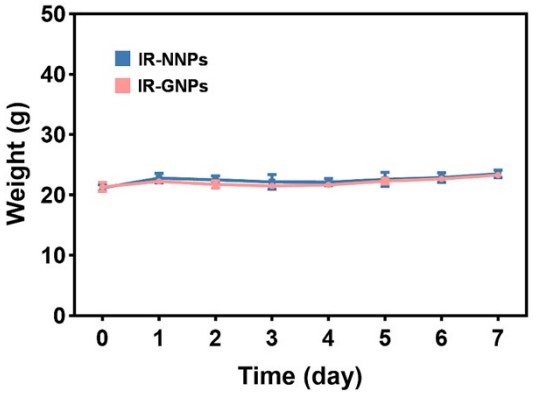

Figure S18. Body weight changes of mice treated with IR-NNPs and IR-GNP at different times. Bars express SD (n = 3).

Table S1. Encapsulation efficiency and loading efficiency of B-NNPs and B-GNPs.

Group	Encapsulation Efficiency (%)	Loading Efficiency (%)
B-NNPs	88.06 ± 2.58	1.73 ± 0.05
B-GNPs	84.87 ± 1.88	1.67 ± 0.04

Table S2. Encapsulation efficiency and loading efficiency of IR-NNPs and IR-GNPs.

Groups	Encapsulation Efficiency (%)	Loading Efficiency (%)
IR-NNPs	86.9 ± 1.77	4.16 ± 0.07
IR-GNPs	87.3 ± 3.21	4.17 ± 0.14

References

1. E. Lepeltier, C. Bourgaux and P. Couvreur, Nanoprecipitation and the "Ouzo effect": Application to drug delivery devices, *Adv. Drug Delivery Rev.*, 2014, **71**, 86-97.

2. S. Schubert, J. T. Delaney and U. S. Schubert, Nanoprecipitation and nanoformulation of polymers: from history to powerful possibilities beyond poly(lactic acid), *Soft Matter*, 2011, **7**, 1581-1588.

3. M. Mu, H. Chen, R. Fan, Y. Wang, X. Tang, L. Mei, N. Zhao, B. Zou,A. Tong, J. Xu, B. Han, G. Guo. A Tumor-Specific Ferric-Coordinated Epigallocatechin-3-gallate cascade nanoreactor for glioblastoma therapy. *J. Adv. Res.* 2021, **30**, 29-41.

4. A. Guo, H. Zhang, H. Li, A. Chiu, C. Garcia-Rodriguez, C. F. Lagos, J. C. Saez and C. G. Lau, Inhibition of connexin hemichannels alleviates neuroinflammation and hyperexcitability in temporal lobe epilepsy, *Proc. Natl. Acad. Sci. U. S. A.*, 2022, **119**, e2213162119.

5. D. F. He, D. L. Ma, Y. C. Tang, J. Engel, Jr., A. Bragin and F. R. Tang, Morpho-physiologic characteristics of dorsal subicular network in mice after pilocarpine-induced status epilepticus, *Brain Pathol.*, 2010, **20**, 80-95.

6. Z. Wang, L. Zhou, D. An, W. Xu, C. Wu, S. Sha, Y. Li, Y. Zhu, A. Chen, Y. Du, L. Chen and L. Chen, TRPV4-induced inflammatory response is involved in neuronal death in pilocarpine model of temporal lobe epilepsy in mice, *Cell Death Dis.*, 2019, **10**, 386.

7. L. Ulmann, F. Levavasseur, E. Avignone, R. Peyroutou, H. Hirbec, E. Audinat and F. Rassendren, Involvement of P2X4 receptors in hippocampal microglial activation after status epilepticus, *Glia*, 2013, **61**, 1306-1319.

8. E. Avignone, L. Ulmann, F. Levavasseur, F. Rassendren and E. Audinat, Status epilepticus induces a particular microglial activation state characterized by enhanced purinergic signaling, *J. Neurosci.*, 2008, **28**, 9133-9144.

9. G. P. Michanetzis, E. Markoutsa, S. Mourtas, Y. F. Missirlis and S. G. Antimisiaris, Hemocompatibility of Amyloid and/or Brain Targeted Liposomes, *Future Med. Chem.*, 2019, **11**, 693-705.

10. X. W. Yu, K. Pandey, A. C. Katzman and C. M. Alberini, A role for CIM6P/IGF2 receptor in memory consolidation and enhancement, *Elife*, 2020, **9**, e54781.

11. J. Chen, T. Wang, Y. Zhou, Y. Hong, S. Zhang, Z. Zhou, A. Jiang and D. Liu, Microglia trigger the structural plasticity of GABAergic neurons in the hippocampal CA1 region of a lipopolysaccharide-induced neuroinflammation model, *Exp. Neurol.*, 2023, **370**, 114565.